

High-power Er:YAG laser at 1646nm pumped by an Er,Yb fiber laser

Peter Jander, Jayanta K. Sahu and W. Andrew Clarkson

Optoelectronics Research Centre, University of Southampton
Southampton, SO17 1BJ, United Kingdom

ABSTRACT

In this paper we describe an Er:YAG laser pumped by a tunable, cladding-pumped Er,Yb fiber laser and discuss factors affecting the laser performance. Crystals with different Er^{3+} -concentrations in the range 0.5% to 4 at% and with crystal lengths selected for ~95% absorption of the pump light at 1532nm were used, and the laser performance was investigated for a range of output coupler transmissions (2-30%) at 1646nm. In preliminary experiments we have achieved a maximum output power of 4W at 1646nm for 11W of absorbed pump power corresponding to an efficiency of 36%, using a crystal with 0.5at% Er^{3+} -concentration and an output coupler transmission of 10%. Our experiments have revealed that the cw efficiency decreases quite markedly for higher Er^{3+} -concentrations. The origin this behaviour is currently the subject of a detailed experimental investigation and our preliminary findings will be presented. The prospects for further increase in output power and efficiency will also be discussed.

1. INTRODUCTION

High-power solid-state lasers operating in the eyesafe wavelength regime around ~1.5-1.6 μm regime have numerous applications and provide an ideal platform for nonlinear frequency conversion to the mid-infrared. The standard approach for producing laser output in this wavelength region is via diode pumping of erbium-ytterbium co-doped bulk glass or crystal lasers [1]. However, due to the short wavelength of the diode pump source (typically ~980nm) compared to the lasing wavelength (~1.5-1.6 microns), these lasers suffer from the problem that large fraction of the pump power is converted to heat in the bulk laser material. This leads to strong thermal lensing, which can severely degrade laser beam quality and efficiency, and to thermally-induced stress, which can cause catastrophic failure of the bulk material. A further problem is that, due to the poor beam quality of the diode pump source, it is necessary to use bulk material with relatively high Er and Yb concentrations. This has the effect of increasing energy-transfer-upconversion, which leads to increased thermal loading and a reduced energy storage time with the result that the laser efficiency is reduced. This problem is especially pronounced when operating the laser in Q-switched (pulsed) mode, due to the higher excitation densities, and can lead to a very significant reduction in the laser pulse energy.

Another approach for producing laser emission in the required wavelength regime is via cladding-pumping of an erbium-ytterbium co-doped fiber laser [2]. Fiber lasers have recently attracted much interest due to their high efficiency, and immunity from thermal effects, and are rapidly emerging as an attractive replacement to conventional bulk solid-state lasers for applications requiring high-power cw output. However, due to their long device length and small core size, fiber lasers suffer from detrimental nonlinear effects, especially when operating in the high peak power pulsed regime, which can limit efficiency. Furthermore, pulse energies are generally limited by amplified spontaneous emission and/or parasitic lasing and ultimately by intensity-induced damage to the fiber end facets.

In this paper, we investigate an alternative approach for efficiently generating high-power output in the ~1.6 μm regime by employing a fiber-bulk hybrid laser scheme which combines the advantages of efficient cw high-power generation in cladding-pumped fiber lasers with the energy storage and high pulse energy capabilities of bulk solid-state laser crystals. The fiber-bulk hybrid laser scheme offers many potential advantages over laser systems based only on 'bulk' or fiber

laser technology. The rationale behind the combination of fiber and bulk technologies in a hybrid laser system is as follows: Firstly, diode-pumping of an Er,Yb co-doped double-clad fiber laser allows the production of high-power cw output in the $\sim 1.5\mu\text{m}$ wavelength regime suitable for direct ‘in-band’ pumping of a bulk Er-doped crystal. This has the important advantage over direct pumping of the bulk Er-doped crystal with a diode, that most of the heat generated via quantum defect heating (typically $\sim 40\%$) is deposited in the fiber, with only $\sim 6\text{--}7\%$ of the fiber laser output power converted to heat in the bulk crystal. The net result is that thermal effects in the bulk Er laser are dramatically reduced leading to the prospect of much improved efficiency, beam quality and higher output power. The fiber laser benefits from a geometry that allows relatively simple thermal management with the generated heat dissipated over a long device length (typically at least a few metres), thereby reducing the likelihood of thermally-induced damage. Furthermore, the output beam quality is determined by the waveguiding properties of the active-ion-doped core with little, if any, impact on beam quality due to thermal lensing. Also, by employing an in-fiber Bragg grating or an external cavity with wavelength-dependent feedback provided by a simple diffraction grating, the Er,Yb fiber laser’s wavelength can be tuned to precisely coincide with the strongest absorption line in the bulk Er material. This is facilitated in a glass host due to the very broad emission spectrum. The combination of good beam quality and wavelength tunability, provided by the fiber laser, also allows the use of long bulk crystals with low erbium concentrations. This reduces the deleterious effects of upconversion allowing long energy storage times and hence in principle high pulse energies can be achieved for relatively modest pump powers. This approach has already been successfully applied to Er:YAG [3] and Er:LuAG [4] lasers pumped (in-band) by an erbium fiber laser, with multi-watt average powers and slope efficiencies with respect to incident pump power up to 54% and 40% respectively. It is worth noting that a similar fiber-bulk hybrid laser approach applied to a Ho:YAG laser pumped by a Tm fiber laser has resulted in even higher slope efficiency ($\sim 80\%$) [5] in spite of a higher quantum defect ($\sim 9\%$).

Here we describe an Er:YAG laser pumped by a tunable, cladding-pumped Er,Yb fiber laser and discuss factors affecting the laser performance. In preliminary experiments we have achieved a maximum output power of 4W at 1646nm for 11W of absorbed pump power corresponding to an efficiency of 36%, using a crystal with 0.5at% Er^{3+} -concentration and an output coupler transmission of 10%. Our experiments indicate that the cw efficiency decreases quite markedly for higher Er^{3+} -concentrations. The origin this behaviour and the prospects for further increase in output power and efficiency are discussed.

2. ERBIUM FIBER LASER

2.1 Diode Pump Source

The Er,Yb fiber laser used in our experiments was constructed in-house and pumped by a high-power diode-stack. At present, diode-stacks provide the highest output power of any commercially available diode source and hence are potentially attractive as pump sources for scaling fiber lasers to high power levels. However, the main disadvantage of diode-stacks is the poor quality and unfriendly nature of their output beams. The beam propagation factor parallel to the diode array, M_x^2 , is typically ~ 2000 , and is many times larger than the beam propagation factor, M_y^2 (after fast-axis collimation), in the stacking direction, making it difficult to focus to the small beam sizes required for efficient cladding pumping. To solve this problem we have employed a two-mirror beam-shaper [6] to reduce the mismatch in the M^2 parameters in orthogonal planes without significantly degrading the brightness. The diode pump source and beam conditioning optics are shown schematically in Fig. 1. A single diode-stack (four-bar) with a maximum cw output power of 160W at $\sim 940\text{nm}$ (purchased from DILAS DiodenLaser GmbH) was employed in our experiments. The output from each bar on the stack was first collimated by a high numerical aperture cylindrical microlens (FAC-850 from LIMO GmbH), and then imaged on to the entrance aperture of a two mirror beam-shaper (not shown) via an arrangement of crossed cylindrical lenses, f_1 and f_3 , and f_2 and f_4 respectively. The lenses were selected to produce a highly elliptical beam with $w_x \gg w_y$, where w_x and w_y are the beam widths in the x and y directions respectively. It is important that the beam width in the y direction is not too small, so that the Rayleigh range is greater than the beam width otherwise there is significant diffraction spreading of the beams in the y-direction as they pass through the beam shaper, leading to a reduction in brightness. To achieve this, focal lengths, $f_1=38\text{mm}$, $f_2=200\text{mm}$, $f_3=150\text{mm}$ and $f_4=40\text{mm}$, were selected to produce a beam of width $\sim 40\text{mm}$ in the x direction and $\sim 1.2\text{mm}$ in the y-direction at the beam-shaper entrance aperture. The beam-shaper mirror spacing and orientation were then selected to slice the incident

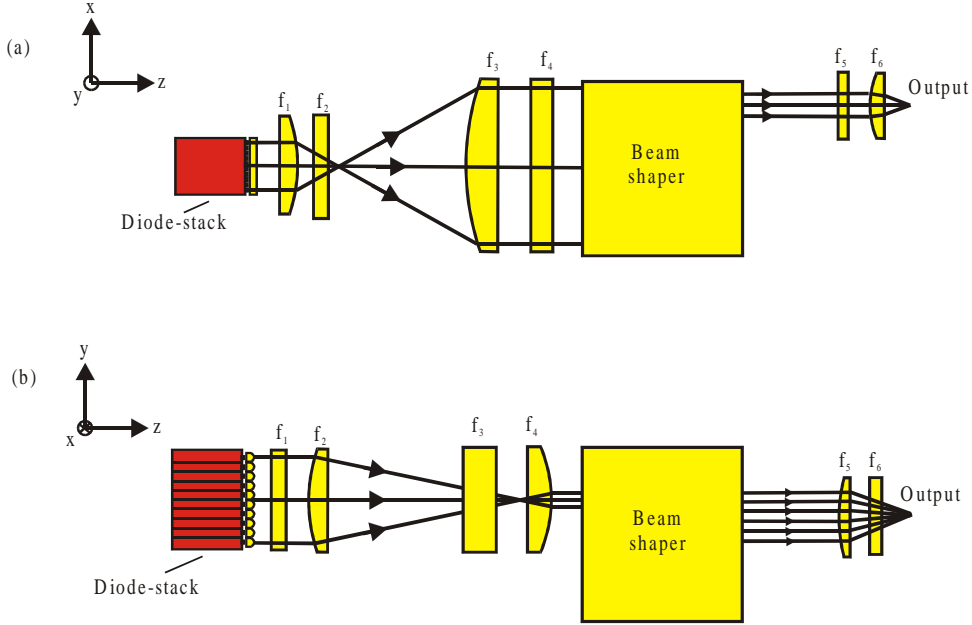


Fig. 1. Diode-stack pump source

beam in the x direction into ~ 11 beams, which were then stacked vertically underneath each other (i.e. in the y direction) by the action of the beam-shaper. Further details of the two-mirror beam-shaper construction and the principle of operation can be found in Ref. 6. The net result was a reduction in the value for M_x^2 and an increase in the value for M_y^2 by a factor ~ 11 . Using this arrangement we obtained final values for the beam quality factors (i.e. after re-shaping) of $M_x^2 \approx 133$ and $M_y^2 \approx 270$ in the x and y directions respectively. The value for M_y^2 was a little larger than expected (due largely to imperfect alignment of the fast-axis collimating lenses) necessitating spatial filtering of the beam (with the aid of the optical arrangement shown in Fig. 2) to reduce the value for M_y^2 by approximately a factor-of-two to allow efficient launching into the Er,Yb-doped double-clad fiber. The combined transmission of the diode-stack collimating and beam re-formating optics was $\sim 87\%$, but was reduced by the spatial filtering arrangement to $\sim 50\%$. The latter reduction in the pump transmission could be avoided with further improvement in the alignment of the fast-axis collimating lenses.

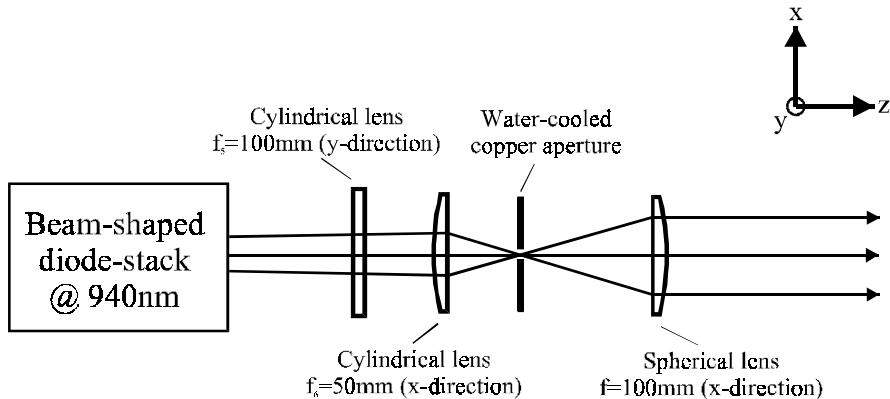


Fig. 2. Spatial filter for diode-stack pump source

2.2 Er,Yb Fiber Laser Design and Performance

The Er,Yb co-doped double-clad fiber (EYDF) used in our experiments was pulled from a preform fabricated in-house using the standard chemical vapour deposition and solution doping technique. The resulting fiber had a slightly multimode phospho-silicate core of 24 μm diameter and a numerical aperture (NA) of 0.21 (i.e. $V\approx 10$) doped with erbium and ytterbium. The inner-cladding was fabricated from pure silica with an outer dimension $\sim 400\mu\text{m}$ and had a D-shaped cross-section to promote efficient pump absorption. The latter was coated with a low refractive index ($n=1.375$) UV curable polymer outer-cladding to produce a high numerical aperture waveguide (calculated as 0.49) for the pump, and hence facilitate efficient launching of pump light from our high-power (but low-brightness) diode source. A target operating wavelength of 1532nm for the Er,Yb-doped double-clad fiber laser (EYDFL) was needed to match the absorption peak in Er:YAG. This is in the short wavelength end of the gain spectrum and hence is more challenging to obtain from a cladding-pumped fiber laser configuration due to the relatively long fiber length required for efficient pump absorption, which results in reduced gain at shorter wavelengths due to increased re-absorption loss and amplified spontaneous emission and /or parasitic lasing at longer wavelengths where the gain is higher. The situation is further exacerbated by the use of a pump wavelength of 940nm for which Yb absorption is much lower than at 975nm (see Fig. 3). To alleviate this problem, a relatively high Yb³⁺ ion concentration of approximately $8.7\times 10^{20}\text{cm}^{-3}$ was used to achieve a relatively high effective pump absorption coefficient of $\sim 1.7\text{dB/m}$ and to promote efficient energy transfer from Yb³⁺ to Er³⁺, and a relatively low Er³⁺ ion concentration ($\sim 5.1\times 10^{19}\text{cm}^{-3}$) to reduce the re-absorption loss at short wavelengths around 1532nm.

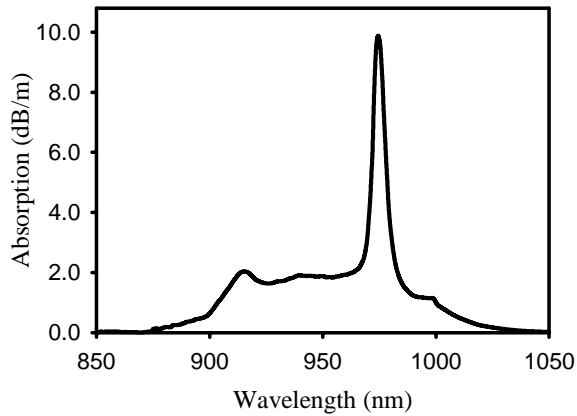


Fig. 3. Absorption in Er,Yb-doped double-clad fiber versus pump wavelength

The EYDFL (shown in Fig. 4) employed a simple tunable cavity design consisting of a 2.6m length of EYDF with feedback for lasing provided by the $\sim 3.6\%$ Fresnel reflection from a perpendicularly-polished fiber end-facet at the pump in-coupling end of the fiber, and at the other end by an external cavity comprising an anti-reflection coated collimating lens of focal length, 120mm, and a diffraction grating with 600 lines/mm mounted on a copper substrate to facilitate removal of waste heat. The grating was blazed for a wavelength of $\sim 1.65\mu\text{m}$ with reflectivity $\sim 75\%$ for light polarised parallel to the grooves and $\sim 95\%$ for light polarised in the orthogonal direction, and was aligned in the Littrow configuration to provide wavelength selective feedback and hence the means for adjusting the lasing wavelength. The fiber end facet nearest the external cavity was angle-polished at $\sim 12.5^\circ$ to the fiber axis to suppress broadband feedback, which might otherwise limit the wavelength tuning range. The perpendicularly-polished fiber end-facet acted as the output coupler with its high transmission dominating other sources of cavity loss. Both end sections of the EYDF (\sim few cm long) were actively-cooled by clamping the fiber between water-cooled copper plates, but the remainder of the fiber was passively cooled. The EYDF was pumped by the diode-stack pump source described in the previous section, with pump and EYDFL output separated with the aid of a dichroic with high reflectivity (at 45°) at the pump wavelength

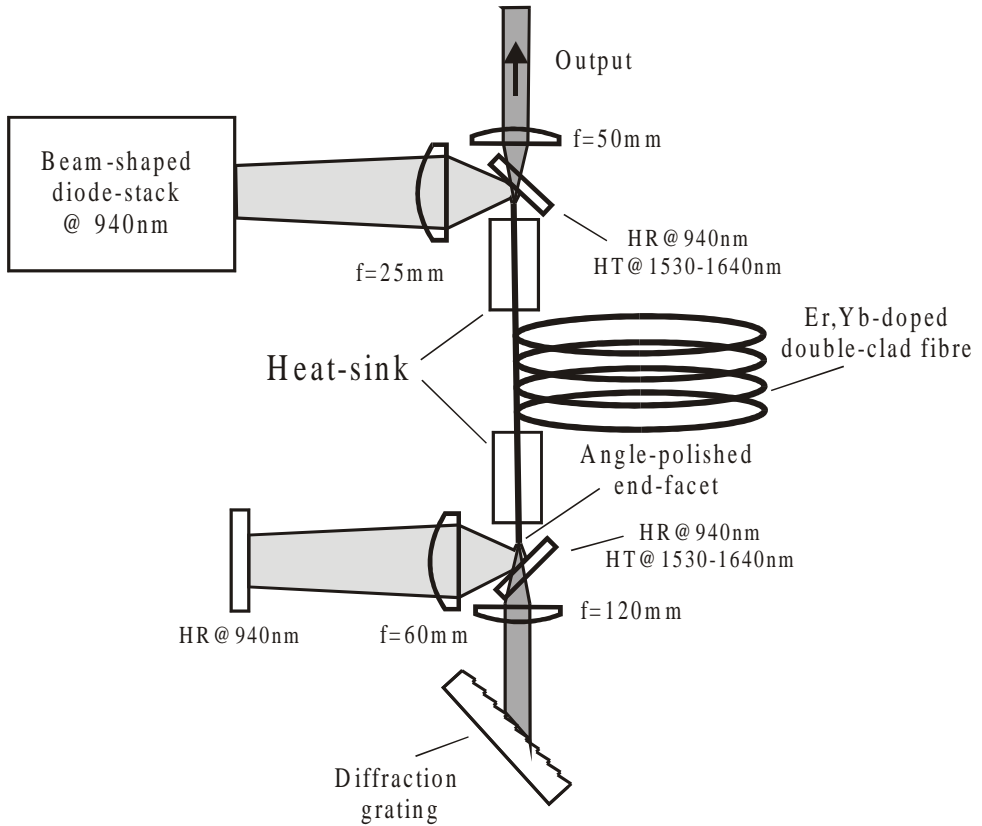


Fig. 4. Tunable Er,Yb fiber laser arrangement

and high transmission at ~ 1500 - 1600 nm. Using this arrangement, a maximum pump power of ~ 54 W was launched into the fiber. The single-pass pump absorption was only $\sim 64\%$, and so the unabsorbed pump light was returned for a second-pass (using the pump feedback scheme shown in Fig. 4) to increase the pump absorption efficiency.

The EYDFL yielded an output power of 18W at 1532nm limited by the maximum available pump power, and the slope efficiency with respect to launched power was $\sim 36\%$ (see Fig. 5). A higher slope efficiency ($\sim 46\%$) with respect to absorbed pump power was achieved with a single-pass pumping configuration indicating that the arrangement for retro-reflecting the unabsorbed pump light after a single-pass is not optimum. Thus, with an improved design there is scope for a significant improvement in the overall efficiency. The linewidth of the EYDFL emission was <0.1 nm and hence much less than the width of the absorption line (~ 1 - 2 nm) in Er:YAG as required for efficient pumping of an Er:YAG laser. The latter was achieved in spite of the slightly multimode nature of the output beam ($M^2=2.5$) by employing a relatively long focal length collimating lens (~ 120 mm) in the external feedback cavity to reduce the collimated beam divergence and hence increase the spectral selectivity of the grating feedback cavity. The operating wavelength was very stable with <0.1 nm drift over a period of several weeks. Moreover, the output power was also very stable with power fluctuations of $<4\%$ over a time period of 20 minutes.

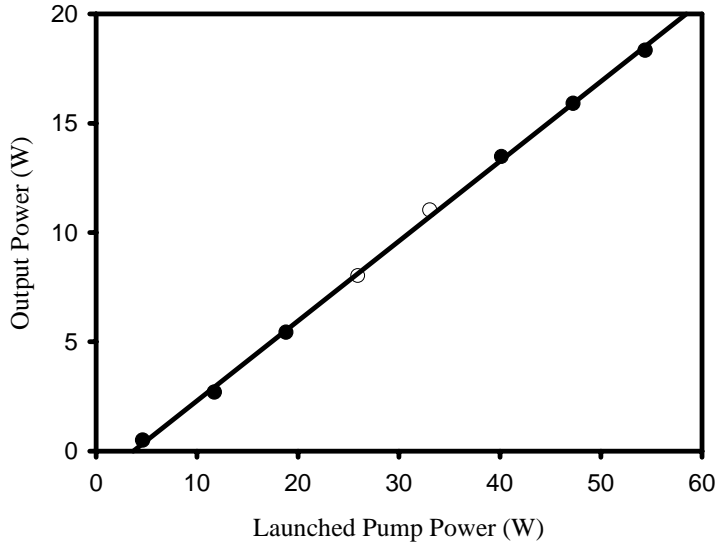


Fig. 5. Er,Yb fiber laser output power at 1532nm versus pump power

3. FIBER LASER PUMPED Er:YAG LASER

Er:YAG is a promising laser material for high-power continuous-wave operation and for the production of high Q-switched pulse energies in the $\sim 1.6\mu\text{m}$ regime owing to its robust thermo-mechanical properties and the long fluorescence lifetime ($\sim 6.5\text{ms}$) [7] for the upper laser manifold (${}^4\text{I}_{13/2}$). A further attractive feature is that it is possible to pump directly into the upper manifold owing to a strong absorption peak at 1532nm which is conveniently accessible by high-power Er-doped fiber sources (see Fig. 6). This suggests that the heat loading in Er:YAG should be very low due to the small quantum defect ($\sim 7\%$), opening up the prospect of very high lasing efficiencies. One of the main objectives of this work was to investigate how various factors (and in particular Er doping concentration) affect laser performance to allow a design strategy to be formulated.

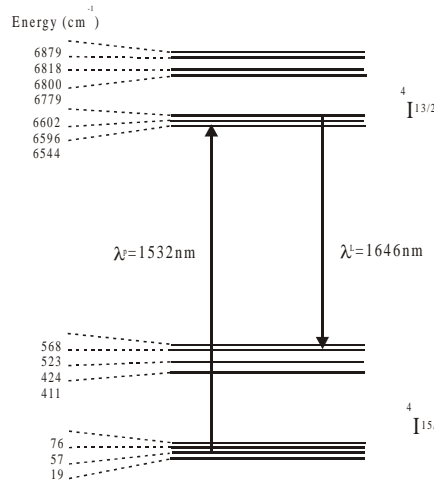


Fig. 6. Energy level diagram for Er:YAG at 300K [8]

3.1 Er:YAG Resonator Design

The experimental arrangement used in our study is shown in Fig. 7. A simple three-mirror folded-cavity design was used for the Er:YAG laser comprising a plane pump in-coupling mirror with high transmission (>95%) at the pump wavelength and high reflectivity (>99.8%) at the lasing wavelength (1646nm), a concave folding mirror with radius of curvature, 100mm, and high reflectivity in the 1560-1680nm regime, and a plane output coupler. Laser performance was evaluated for Er:YAG rods with Er³⁺ doping levels of 0.5at.%, 1at.%, 2at.% and 4at.% and respective lengths of 29mm, 15mm, 7.3mm and 3.8mm, which were selected to be approximately equal to three absorption lengths for pump light at 1532nm. The laser rods had a diameter of 2mm (4mm for the 0.5at.% Er:YAG rod) and had antireflection coatings for the wavelength range, 1.5-1.7μm, on both end faces. In each case the Er:YAG crystal was mounted in a water-cooled copper heat-sink with the cooling water maintained at a temperature of ~15°C, which was positioned ~0.5mm from the pump in-coupling mirror. The optical path lengths from the input coupler to the concave mirror and from the concave mirror to the output coupler were selected to be 57mm and 165mm respectively. This arrangement resulted in a TEM₀₀ mode radius in the Er:YAG rod of 75μm, which was relatively insensitive to the thermal lensing over the range of pump powers used. Pump light from the EYDFL was collimated by a 50mm focal length plano-convex lens and focused to a pump beam waist radius, w_p, in the Er:YAG crystal of ~114μm using a 250mm plano-convex lens. This resulted in relatively long Rayleigh range (z_{op}=πnw_p²/M²λ) of ~19mm and hence little diffraction spreading of the pump beam even in the longest crystal.

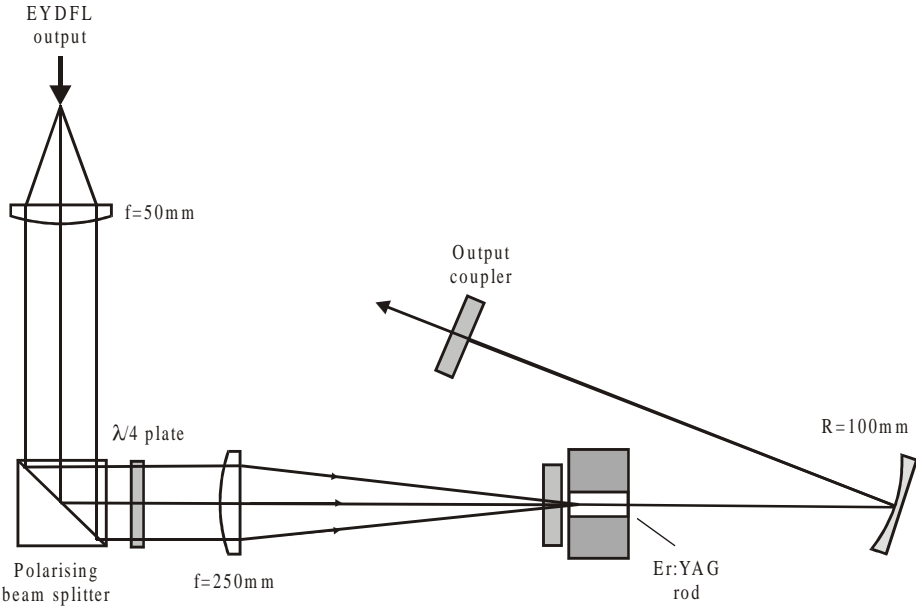


Fig. 7. Er:YAG laser set-up

In preliminary experiments no attempt was made to isolate the EYDFL from feedback from the Er:YAG laser. However, the Er:YAG cavity can act as an external feedback cavity for the EYDFL at wavelengths outside the Er:YAG absorption band and hence competes with the wavelength selection provided by the diffraction grating. The net result of this feedback was that the EYDFL tended to operate at longer wavelengths to avoid the strong absorption peak in Er:YAG at 1532nm unless care was taken to carefully optimise the alignment of the EYDFL's grating feedback cavity to dominate over this wavelength selection mechanism. As an extra precaution against tuning of the EYDFL wavelength away from the Er:YAG absorption line, a simple isolator comprising a polarizer and quarter-wave plate was placed in the pump beam path between the collimating and focusing lenses for most of our experiments. This had the undesirable effect of reducing the available incident pump power from ~14W to ~6.5W, since the EYDFL output was

not polarised. However, this proved to be a sufficient power level for our investigation into the effect of Er concentration on Er:YAG laser performance.

3.2 Er:YAG Laser Performance

The best performance was obtained using the 0.5at.% Er-doped crystal, which produced a maximum output power of ~1.6W at 1646nm for ~5W of absorbed pump power at 1532nm, using an output coupler with transmission ~10%. In contrast, under the same experimental operating conditions (i.e. at the same pump power and using the same output coupler) lasers employing the 1.0at.% and 2.0at.% doped crystals produced only 1.3W and 0.56W of output respectively. Moreover, and in spite of many attempts, it was not possible to reach threshold for laser oscillation with the 4at.% doped crystal. The situation is more clearly illustrated in Fig. 8 and Fig. 9, which show, respectively, the dependence of threshold pump power and slope efficiency on Er concentration for different output couplers with

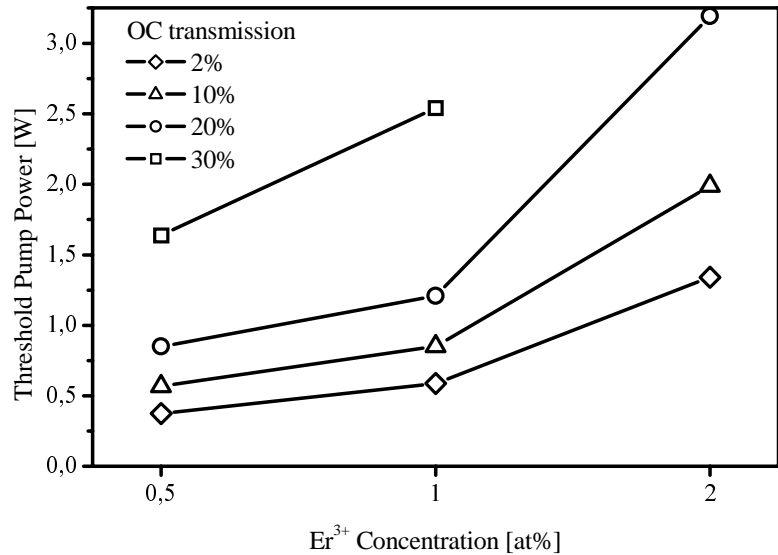


Fig. 8. Er:YAG threshold pump power versus Er concentration

transmissions at 1646nm of 2%, 10%, 20% and 30%. It can be seen that there is a dramatic increase in the threshold pump power and a decrease in the slope efficiency, which cannot be explained by an increase in cavity loss, since the losses for the Er:YAG rods (i.e. excluding re-absorption loss) were estimated to be very low (<1%) and hence in-line with our expectations based residual reflectivity of the antireflection coatings on the end faces. The 1646nm ($^4I_{13/2} \rightarrow ^4I_{15/2}$) transition in Er:YAG is a quasi-three-level transition since the lower laser level resides in the ground state manifold. An approximate value for the threshold pump power, P_{pth} , can be calculated from [9]:

$$P_{\text{pth}} \approx \frac{\pi h v_p (w_p^2 + w_L^2) (L + T + 2f_1 \sigma N_l L_c)}{4f_2 \sigma \tau_f \eta_{\text{abs}}} \quad (1)$$

where L_c is the length of the laser rod, w_p is the pump beam radius in the laser rod, w_L is the TEM₀₀ mode radius in the laser rod, L is the cavity loss, T is the transmission of the output coupler, N_l is the population of the lower manifold, τ_f is the lifetime of the upper laser level, η_{abs} is the fraction of the incident pump power absorbed, and f_1 and f_2 are the fractions of the populations of the lower and upper level manifolds which reside in the lower and upper laser level respectively. At room temperature, $f_1 \approx 0.02$ and $f_2 \approx 0.21$, hence ~8.7% of the Er ions must be excited to reach transparency. Taking $\sigma = 2 \times 10^{-20} \text{ cm}^2$ and assuming that the round-trip cavity loss (excluding the output coupling loss) is ~1%, we estimate from equation (1) that the threshold pump power for our Er:YAG laser with an output coupler

transmission of $\sim 10\%$ is $\sim 0.2\text{W}$ and is independent of the Er concentration. The latter results from the fact that N_1L_c is approximately the same for all of the rods investigated. It is worth noting that just over half this threshold power is required to reach transparency. The calculated threshold is much lower than we achieve in practice even for the lowest Er concentration. The fact that the threshold pump power increases so dramatically with Er concentration is a very surprising result. A preliminary investigation into the effect of energy-transfer upconversion on laser performance, via the process $(^4\text{I}_{13/2} \rightarrow ^4\text{I}_{15/2}) + (^4\text{I}_{13/2} \rightarrow ^4\text{I}_{9/2})$, has been conducted and indicates that upconversion has a relatively small effect on the cw threshold for doping levels below 2at.% and for cavity losses less than $\sim 10\%$. Thus, upconversion does not account for the strong increase in threshold with increasing Er concentration observed experimentally. Moreover, it cannot explain the decrease in slope efficiency with increasing Er concentration. Clearly, further studies are needed to identify the mechanism for the decrease in lasing efficiency with increasing Er concentration.

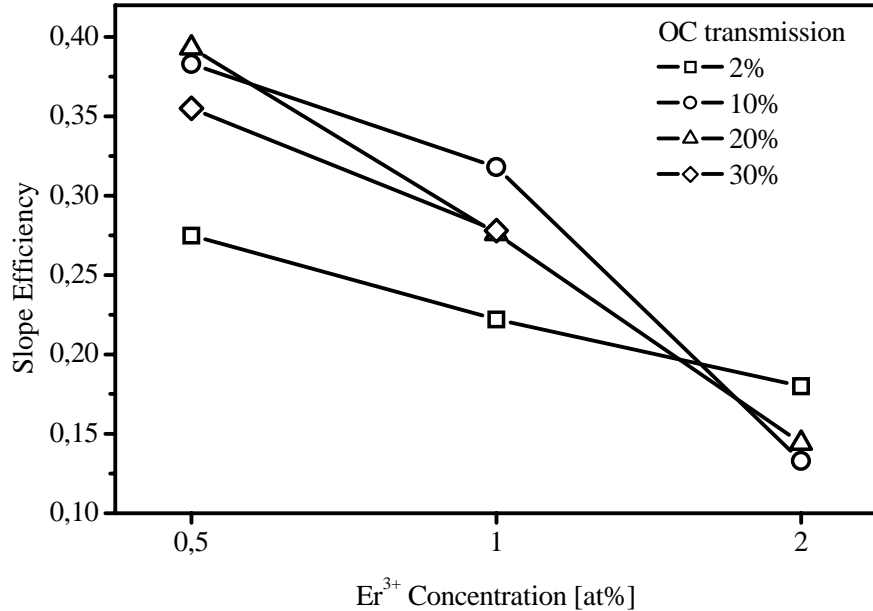


Fig. 9. Er:YAG slope efficiency versus Er concentration

The lowest threshold and highest slope efficiency were obtained using the Er:YAG rod with lowest Er concentration of 0.5at.%. By removing the isolator from our set-up to increase the available pump power and by carefully aligning the diffraction grating to ensure that the EYDFL operated at 1532nm we were able to increase the output power from the 0.5at.% doped Er:YAG laser with a 10% transmitting output coupler to 4.2W for 11.5W of incident pump power (see Fig. 10, in a nearly diffraction-limited TEM₀₀ beam with $M^2 \approx 1.2$). The slope efficiency with respect to absorbed pump power was a little higher ($\sim 44\%$) than was achieved with lower pump powers, but still much lower than one would expect based on the very low quantum defect.

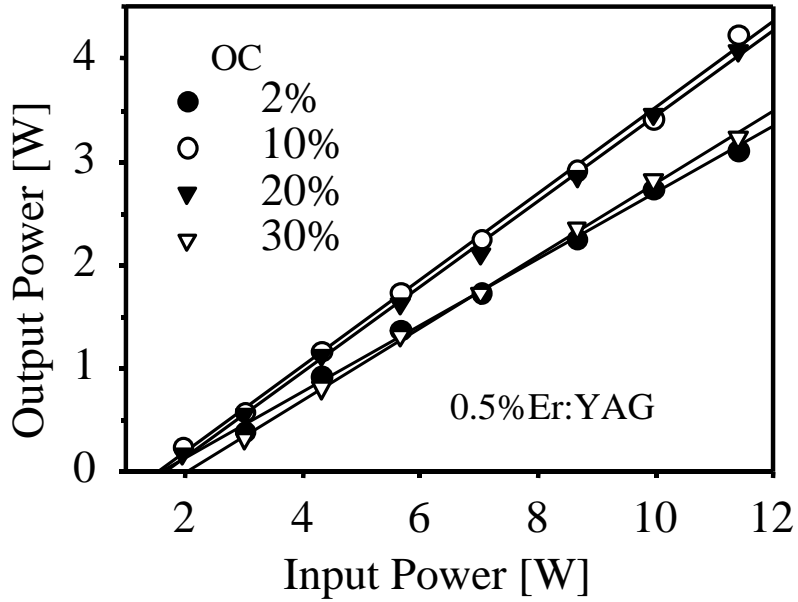


Fig. 10. Output power versus incident pump power for 0.5at.% doped Er:YAG laser

4. SUMMARY AND CONCLUSIONS

In-band pumping of an Er:YAG laser by a cladding-pumped Er,Yb fiber laser has been investigated. Using a 0.5at.% doped Er:YAG rod we obtained a maximum output power of $\sim 4.2\text{W}$ (limited by available pump power) in a TEM_{oo} beam with $M^2 \approx 1.2$. The slope efficiency with respect to absorbed pump power was $\sim 44\%$. We have found that the efficiency of Er:YAG lasers operating on the 1646nm is strongly dependent on the Er^{3+} concentration. In comparable laser configurations we observed a dramatic decrease in threshold and increase in slope efficiency by reducing the Er concentration from 2% to 0.5%. This is a very surprising result given that the lasers were all operated in cw mode and had relatively small cavity losses. Energy-transfer-upconversion has been investigated as a possible mechanism for this behaviour. Our results indicate that upconversion does play an important role and should certainly be taken into account when high excitation densities are involved (i.e. in Q-switched lasers or cw lasers with high cavity losses), but does not account for the observed concentration dependence of performance in our experiments. There is clearly an additional mechanism (as yet unidentified) which has a very detrimental effect on efficiency and is strongly dependent on Er concentration. It seems likely that a further reduction in the Er doping level may well lead to a further improvement in efficiency.

5. ACKNOWLEDGEMENTS

This work was funded by the EOARD under contract number F61775-01-C0008.

6. REFERENCES

1. A. Levoshkin, A. Petrov and J. E. Montagne, "High-efficiency diode-pumped Q-switched Yb:Er:glass laser," Opt. Comm., **185**, pp.399-405, 2000.
2. J. K. Sahu, Y. Jeong, D. J. Richardson and J. Nilsson, "A 103W erbium-ytterbium co-doped large-core fiber laser," Opt. Comm., **227**, pp.159-163, 2003.
3. Y. E. Young, S. D. Setzler, K. J. Snell, P. A. Budni, T. M. Pollak and E. P. Chicklis, "Efficient 1645nm Er:YAG laser," Opt. Lett., **29**, pp.1075-1077, 2004.
4. S. D. Setzler, K. J. Snell, T. M. Pollak, P. A. Budni, Y. E. Young and E. P. Chicklis, "5W repetitively Q-switched Er:LuAG laser resonantly pumped by an erbium fiber laser," Opt. Lett., **28**, pp.1787-1789, 2003. p.1787.
5. D. Y. Shen, A. Abdolvand, L. J. Cooper and W. A. Clarkson, "Efficient Ho:YAG laser pumped by a cladding-pumped tunable Tm:silica-fibre laser," Appl. Phys. B, **79**, pp.559-561, 2004.
6. W. A. Clarkson, and D.C. Hanna, "Two-mirror beam-shaping technique for high-power diode bars", Opt. Lett. **21**, pp.375-377, 1996.
7. H. Strange, K. Petermann, G. Huber and E. W. Duczynski, "Continuous-wave 1.6 μ m laser action in Er doped garnets at room temperature," Appl. Phys. B., **49**, pp.269-273, 1989.
8. K. Spariosu and M. Birnbaum, "Intracavity 1.549 μ m pumped 1.634 μ m Er:YAG lasers at 300K," IEEE J. Quantum Electron., **30**, pp.1044-1049, 1994.
9. T. Y. Fan and R. L. Byer, "Modeling and cw operation of a quasi-three-level 946nm Nd:YAG laser," IEEE J. Quantum Electron., **23**, pp.605-612, 1987.